COPY

AD-A221 618

AD

TECHNICAL REPORT ARCCB-TR-90011

LOAD-POINT COMPLIANCE FOR
THE ARC BEND-ARC SUPPORT
FRACTURE TOUGHNESS SPECIMEN

FRANCIS I. BARATTA

JOSEPH A. KAPP

DAVID S. SAUNDERS

DTIC
ELECTE
MAY 11 1990
S B D

MARCH 1990

90 05 11 048

DISCLAIMER

The findings in this report are not to be construed as an official Department of the Army position unless so designated by other authorized documents.

The use of trade name(s) and/or manufacturer(s) does not constitute an official indorsement or approval.

DESTRUCTION NOTICE

For classified documents, follow the procedures in DoD 5200.22-M, Industrial Security Manual, Section II-19 or DoD 5200.1-R, Information Security Program Regulation, Chapter IX.

For unclassified, limited documents, destroy by any method that will prevent disclosure of contents or reconstruction of the document.

For unclassified, unlimited documents, destroy when the report is no longer needed. Do not return it to the originator.

REPORT DOCUMENTATION PAGE		READ INSTRUCTIONS BEFORE COMPLETING FORM
1. REPORT NUMBER ARCCB-TR-90011	2. GOVT ACCESSION NO.	3. RECIPIENT'S CATALOG NUMBER
4. TITLE *(and Subtitle)* LOAD-POINT COMPLIANCE FOR THE ARC BEND-ARC SUPPORT FRACTURE TOUGHNESS SPECIMEN		5. TYPE OF REPORT & PERIOD COVERED Final
		6. PERFORMING ORG. REPORT NUMBER
7. AUTHOR(s) Francis I. Baratta, Joseph A. Kapp, and David S. Saunders (See Reverse)		8. CONTRACT OR GRANT NUMBER(s)
9. PERFORMING ORGANIZATION NAME AND ADDRESS U.S. Army ARDEC Benet Laboratories, SMCAR-CCB-TL Watervliet, NY 12189-4050		10. PROGRAM ELEMENT, PROJECT, TASK AREA & WORK UNIT NUMBERS AMCMS No. 6111.02.H610.011 PRON No. 1A92Z9CANMSC
11. CONTROLLING OFFICE NAME AND ADDRESS U.S. Army ARDEC Close Combat Armaments Center Picatinny Arsenal, NJ 07806-5000		12. REPORT DATE March 1990
		13. NUMBER OF PAGES 35
14. MONITORING AGENCY NAME & ADDRESS(*If different from Controlling Office*)		15. SECURITY CLASS. *(of this report)* UNCLASSIFIED
		15a. DECLASSIFICATION/DOWNGRADING SCHEDULE

16. DISTRIBUTION STATEMENT *(of this Report)*

Approved for public release; distribution unlimited.

17. DISTRIBUTION STATEMENT *(of the abstract entered in Block 20, if different from Report)*

18. SUPPLEMENTARY NOTES

Presented at the 21st National Fracture Mechanics Symposium, Annapolis, MD, June 1988.
Published in Proceedings of the Symposium - ASTM STP.

19. KEY WORDS *(Continue on reverse side if necessary and identify by block number)*

Fracture Mechanics, ASTM Standard E-399, Mechanics, Physics,
Fracture Testing,   Arc-Support Flexure,
Stress Intensity Factors
Numerical Stress Analysis,
Compliance

20. ABSTRACT *(Continue on reverse side if necessary and identify by block number)*

The primary objective of this work is to provide the theoretical computation of load-point compliance for the arc bend-arc support specimen and some experimental verification of these predictions. This specimen is a segment of an annular disk loaded in three-point bending with the roller supports positioned at the inside surface.

(CONT'D ON REVERSE)

DD _{1 JAN 73} **1473** EDITION OF 1 NOV 65 IS OBSOLETE

UNCLASSIFIED

7. AUTHORS (CONT'D)

Francis I. Baratta
U.S. Army Materials Technology Laboratory
Watertown, MA 02172

David S. Saunders
Aeronautical Research Laboratories
Melbourne, Victoria 3001
Australia

20. ABSTRACT (CONT'D)

Load-line compliance was determined principally by utilizing Irwin's Equation that relates the compliance rate of change with crack length to the strain energy release rate. The strain energy release rate was determined from the stress intensity solution available in the literature for this sample. Corroboration was also provided by utilizing boundary collocation (BC), boundary integral element (BIE), and finite element methods (FEM). Representative cases were experimentally tested to confirm theoretical and numerical results. During those tests, it was also found that duplication of idealized support and fixture conditions were extremely important with regard to accurate measurement of load-point compliance.

Two statically-equivalent models were used to calculate the load-line compliance using the numerical methods. The first is Model 1, where the load point is fixed and the roller reactions are applied at the appropriate location. The second is Model 2, and in this case, the load is applied at the load point and the roller reaction points are fixed in the appropriate manner. Although both models are statically equivalent, significantly different load-line compliances are obtained depending upon the model chosen.

Experimental results were also obtained. Specimens were tested with machined slots to simulate a crack and other specimens tested had fatigue cracks. The measured compliances agreed with Model 2 results in some cases, with Model 1 in other cases, and with neither in still other cases.

Accession For	
NTIS GRA&I	☑
DTIC TAB	☐
Unannounced	☐
Justification	
By	
Distribution/	
Availability Codes	
Dist	Avail and/or Special
A-1	

TABLE OF CONTENTS

TABLES

LIST OF ILLUSTRATIONS

ACKNOWLEDGEMENTS

INTRODUCTION

The arc-shaped tension loaded (A(T)) specimen has been accepted as one of the standard fracture toughness samples in ASTM Standard E-399 on Fracture Toughness Testing of Metals since 1978. This specimen, which is a single-edge notched and fatigue-cracked ring segment loaded in tension can be easily fabricated from hollow thick-walled cylinders. For some applications, such as relatively thin-walled tubing, a bending sample would be more convenient. Two bending sample variations of the arc-shaped sample have been suggested. One of these is the arc bend-chord support sample where the reaction loads are applied to a chord that is machined in the specimen (Figure 1a). The second type is the arc bend-arc support sample where the reaction loads are applied at the inside diameter of the sample (Figure 1b). This report deals only with the latter sample.

ASTM Task Group E24.01.05 on Fracture Specimen Design considered the distinct advantages the arc bend-chord support sample has as compared to the arc bend-arc support sample. Thus, the arc bend-arc support sample was eliminated from consideration as a standard fracture toughness sample. Nevertheless, useful information has been generated in the analysis of the arc bend-arc support sample, such as the development of stress intensity factor and crack-mouth-opening displacement solutions using boundary collocation (ref 1). This report presents the results of further analyses to calculate and measure the load-line compliance of the arc bend-arc support sample.

The primary load-line compliance results were obtained in the following manner. It is assumed that the total load-line compliance of sample (Δ_{tot}) is given by

$$\Delta_{tot} = \Delta_{crack} + \Delta_{no\ crack} \qquad (1)$$

where $\Delta_{no\ crack}$ is the compliance of the specimen with no crack present and Δ_{crack} is the additional displacement due to the presence of the crack. Using this formulation, $\Delta_{no\ crack}$ is determined using Winkler's theory as referenced by Jones (ref 2), and Δ_{crack} is found by integrating Irwin's compliance equation (ref 3)

$$G = \frac{P^2}{2B} \frac{\partial C}{\partial a} \qquad (2)$$

where G is the strain energy release rate, C is the compliance of the sample ($C = \Delta_{crack}/P$; P being the load), and a is the crack depth. The energy release rate is determined from (ref 4)

$$G = K^2/E' \qquad (3)$$

where K is the stress intensity factor and E' is the elastic modulus (E) for plane-stress conditions or ($E'=E/(1-\mu^2)$; μ being Poisson's ratio) for plane-strain.

In addition, load-line compliance solutions were obtained using boundary collocation (BC), finite element methods (FEM), and the boundary integral element method (BIE). Two different modeling methods were used when these numerical techniques were employed. Also, load-line compliance was measured on several specimen geometries.

LOAD-LINE COMPLIANCE USING IRWIN'S EQUATION

As stated, the load-line compliance can be determined with Eq. (1), obtaining Δ_{crack} by integrating Eq. (2). The formulation of $\Delta_{no\ crack}$ using Winkler's theory, has been accomplished by Jones (ref 2) and is not discussed in detail in this report. The result for $\Delta_{no\ crack}$ is

$$\Delta_{no\ crack} = \frac{P}{BE} \left\{ \frac{k+1}{8(k-1)} \left[\left(\frac{\theta_0}{\cos^2 \theta_0} - \tan \theta_0 \right) / \left(1 - \frac{2(k-1)}{(k+1)\ln(k)} \right) + \frac{(2+3\mu)\theta_0}{\cos^2 \theta_0} \right. \right.$$

$$\left. \left. + (4+3\mu)\tan \theta_0 \right] \right\} \tag{4}$$

where B is the through-thickness, k is the radius ratio (r_2/r_1), and θ_0 is the angle of support.

To determine the value of Δ_{crack}, we use the stress intensity factor solution of Gross and Srawley (ref 1) in Eq. (3) and substitute the result into Eq. (2). Upon rearranging and integrating, the result is

$$\Delta_{crack} = 2\tan^2 \theta_0 \int_0^{a/W} [f(a/W)]^2 d(a/W) \tag{5}$$

$$f(a/W) = \frac{KB(W)^{\frac{1}{2}}}{P \tan \theta_0} \tag{6}$$

where W is the specimen width, and P is the applied load.

Since the stress intensity factor solution developed in Reference 1 is a numerical solution and is reported only at discreet values of (a/W), to evaluate the integral in Eq. (5), the numerical solution must be estimated at values of a/W other than those reported. To do this, interpolating polynomials of the following type were fit to the K solutions:

$$f(a/W) = \frac{KB(W)^{\frac{1}{2}}}{P \tan \theta_0} = A_1 e^{(A_2(a/W) + A_3(a/W)^2 + A_4(a/W)^3)} \tag{7}$$

where A_1, A_2, A_3, and A_4 are constants determined by least squares fitting to the numerical solution and e is the base of the Naperian logarithm. The integration was performed using Simpson's rule. The results for Δ_{total} are

3

given . Table I, for a wide range of radius ratios (r_2/r_1), support angles (θ_0) in degrees, and crack depths (a/W).

TABLE I. E'BΔ_{total}/P DETERMINED USING IRWIN'S EQUATION APPROACH

$r_2/r_1 = 1.1$

a/W \ θ_0	11.46	18	27	36	45	54	63	72	81
0.0	23.27	85.51	302.7	826.7	2006	4729	11770	35130	179100
0.1	25.30	89.90	316.2	854.4	2058	4829	11970	35640	181200
0.2	29.35	100.8	343.7	911.2	2167	5037	12400	36680	185700
0.3	36.50	120.2	392.8	1013	2361	5407	13160	38550	193800
0.4	48.47	152.5	474.8	1182	2685	6025	14420	41680	206700
0.5	69.02	207.7	614.4	1470	3234	7073	16560	46970	229200
0.6	107.9	311.4	874.7	2007	4255	9018	20530	56770	270600
0.7	195.8	543.2	1454	3199	6517	13320	29300	78410	362200
0.8	450.9	1212	3117	6619	12989	25610	54340	140200	587500

$r_2/r_1 = 1.15$

a/W \ θ_0	13.5	18	27	36	45	54	63	72	81
0.0	13.42	29.31	100.2	268.7	646.2	1517	3763	11210	57100
0.1	14.63	31.61	106.0	280.8	669.5	1561	3855	11440	58050
0.2	17.17	36.48	118.6	307.0	719.8	1657	4052	11930	60120
0.3	21.79	45.36	141.5	354.8	811.9	1834	4413	12820	64420
0.4	29.63	60.41	180.2	435.7	967.4	2131	5023	14330	70350
0.5	43.19	86.30	246.3	573.5	1232	2636	6058	16900	81200
0.6	68.97	135.1	370.0	830.4	1724	3572	7975	21630	101300
0.7	127.6	245.3	646.6	1402.8	2815	5646	12210	32090	145600
0.8	301.2	569.0	1453	3066	5977	11640	24430	62220	273300

$r_2/r_1 = 1.2$

a/W \ θ_0	13.5	18	27	36	45	54	63	72	81
0.0	7.12	14.69	47.59	124.9	297.1	693.0	1714	5093	25890
0.1	7.84	16.07	51.14	132.3	311.3	720.6	1769	5232	26480
0.2	9.30	18.91	58.58	147.9	341.5	778.8	1888	5527	27740
0.3	11.94	24.06	72.06	176.2	396.3	884.4	2105	6066	30030
0.4	16.43	32.78	94.92	224.2	488.9	1062	2471	6974	33890
0.5	24.30	47.97	134.3	306.4	647.2	1366	3095	8521	40460
0.6	39.48	76.88	208.5	460.5	943.0	1934	4256	11390	52640
0.7	74.43	142.6	375.3	805.0	1601	3195	6831	17740	79550
0.8	178.1	335.5	860.4	1802	3500	6826	14240	35960	156600

TABLE I.   (CONT'D)

θ_0 a/W	18	27	36	45	54	63	72	81
				$r_2/r_1 = 1.25$				
0.0	9.00	27.59	70.66	166.0	384.5	946.7	2806	14240
0.1	9.92	30.00	75.71	175.8	403.2	985.1	2901	14640
0.2	11.82	35.02	86.29	196.3	442.8	1067	3104	15510
0.3	15.22	44.09	105.5	233.6	514.8	1215	3473	17080
0.4	21.02	59.46	138.0	296.6	636.3	1465	4095	19730
0.5	31.13	86.02	193.7	404.4	843.7	1892	5154	24240
0.6	50.57	136.4	298.8	606.4	1231	2686	7123	32630
0.7	95.24	250.6	535.2	1059	2096	4454	11500	51230
0.8	227.8	586.1	1226	2373	4602	9570	24130	150000

$$r_2/r_1 = 1.5$$

θ_0 a/W	27	36	45	54	63	72	81
0.0	6.500	14.74	32.31	71.72	171.9	500.3	2508
0.1	7.300	16.46	34.59	78.28	185.5	534.4	2654
0.2	8.890	19.94	42.56	91.74	213.5	604.9	2956
0.3	11.71	26.13	54.86	115.8	263.9	731.2	3499
0.4	16.51	36.59	75.58	156.4	348.4	943.1	4409
0.5	24.93	54.79	111.4	226.0	493.2	1305	5957
0.6	41.37	89.77	179.7	357.9	766.4	1986	8855
0.7	79.85	170.5	336.2	657.6	1385	3522	15360
0.8	196.4	412.1	802.0	1545	3210	8033	34420

$$r_2/r_1 = 2.0$$

θ_0 a/W	31.5	36	45	54	63	72	81
0.0	3.33	4.64	9.110	18.69	42.39	118.7	578.4
0.1	3.79	5.32	10.49	21.46	48.18	133.6	643.0
0.2	4.68	6.65	13.23	26.97	59.94	163.5	773.6
0.3	6.24	8.99	18.06	36.68	80.80	216.4	1004
0.4	8.93	12.97	26.22	52.98	115.7	304.6	1386
0.5	13.72	20.02	40.49	81.23	175.7	455.4	2037
0.6	23.32	33.97	68.29	135.6	289.8	741.5	3264
0.7	46.45	67.24	133.7	262.0	551.4	1396	6055
0.8	118.6	170.2	333.7	645.0	1337	3360	14370

TABLE I. (CONT'D)

θ_0						
a/W	36	45	54	63	72	81
0.0	2.88	5.30	10.33	22.46	60.87	289.5
0.1	3.30	6.22	12.20	26.50	71.30	335.4
0.2	4.15	7.99	15.86	34.43	91.87	426.0
0.3	5.61	11.10	22.25	48.24	127.7	583.5
0.4	8.11	16.36	32.95	71.23	186.9	842.8
0.5	12.62	25.65	51.58	110.8	288.0	1282
0.6	21.70	43.94	87.73	186.8	480.3	2111
0.7	43.74	87.47	172.5	362.8	922.5	4001
0.8	112.7	222.0	431.6	896.8	2256	9666

$r_2/r_1 = 2.5$

For completeness, the load-line compliances for the arc bend-arc support specimen with external cracks are considered in the same manner as outlined above, using Irwin's Equation approach. These results are presented in tabular form in Appendix A.

LOAD-LINE DISPLACEMENT SOLUTIONS WITH NUMERICAL METHODS

For analysis purposes, the arc bend-arc support sample can be modeled as shown in Figure 2a, if it is assumed that the roller supports cause a reaction force to act radially as shown. This is probably the case if the displacement of the sample is small. Large displacements cause the inside surface of the specimen to roll over the reaction rollers. This changes the boundary conditions making the problem nonlinear. For this study, small displacements are assumed and a linear analysis is performed. A second model for the specimen is shown in Figure 2b. In this case, the load is applied as in the actual loading of the specimen and the reactions are at the inside radius of the sample. Both of these models are used to determine the load-line displacements.

Three methods were used to develop the load-line displacements: a finite element method (ref 5), a boundary value collocation method (ref 6), and a boundary integral element method (ref 7). The boundary value collocation results are generated using exactly the same stress function and its derivative as reported in Reference 1. In that earlier study, stress intensity factors and crack-mouth-opening displacements only were generated. If only these two parameters are sought, a relatively small boundary is all that is required for the analysis. The stresses that result on a radial plane between the reactions at $\theta = \theta_0$ and $\theta = 0$ can be calculated and applied to that annular segment at the intermediate radial plane. The loading is equivalent to the actual loading and is sufficient to determine stress intensity factors and crack-mouth-opening displacements, but this modeling is not sufficient to determine the load-line displacement. The boundary collocation method used here and in Reference 1 is based on the Williams stress function (ref 6). With this stress function, all displacements are relative to the displacement of the crack tip, or it is assumed that the crack tip is stationary. In order to determine the load-line displacement with this method, the displacement of two points must be known: first, the displacement of the point of applied external force relative to the crack tip, and second, the component of displacement in the direction of the applied external force at the roller reaction. In order to accomplish this, the reaction point must be included on the boundary which is analyzed. The boundaries studied here included the reaction point, which is the only difference between this analysis and that reported in Reference 1.

The finite element method applied here (ref 5) utilizes cubic isoparametric elements and is written such that either model for the specimen can be applied. Grid points at any location can either be loaded or constrained. We used this

7

method to model the problem in both ways described above. In this study, the boundary integral element code used utilized cubic Hermitian elements (ref 7). This code was written so that only entire elements could be constrained or loaded. This makes it difficult to model the loading of the arc bend-arc support sample by loading at the physical load point and reacting the load at the inside radius (the physical reaction point). These loads and reactions are in the ideal case point loads and reactions. Therefore, only the first modeling described with the boundary integral element method was used.

NUMERICAL RESULTS

Solutions were obtained for a wide range of specimen geometries and loading conditions. Since the arc bend-arc support sample can have many radius ratios (r_2/r_1), several reaction points θ_0, and several crack depths (a/W), all of these variables were studied. In the interest of brevity, only a representative number of these solutions are presented here. These are for the cases of r_2/r_1 = 1.1, 1.5, and 2.0 at θ_0 = 36 or 54 degrees and $0.3 \leqslant a/W \leqslant 0.7$. The results are shown in Table II for θ_0 = 36 degrees and in Table III for θ_0 = 54 degrees. Included in the tables are the solutions for the stress intensity factor (K) and the crack-mouth-opening displacement (Δ_{cm}) as well as the load-line displacement. The K and Δ_{cm} solutions are presented to give a measure of the accuracy to the numerical solutions.

TABLE II. NUMERICAL SOLUTIONS FOR THE ARC BEND-
ARC SUPPORT SAMPLE WITH θ_0 = 36 DEGREES

$$\frac{KB\sqrt{W}}{P\ \tan\ \theta_0}$$

Method	r_2/r_1	a/W				
		0.3	0.4	0.5	0.6	0.7
Coll (ref 1)	1.1	34.97	45.32	60.37	84.23	130.9
Coll (TS)	1.1	--	--	--	--	--
BIE	1.1	35.26	45.83	61.28	86.70	135.8
FM (ARF)	1.1	34.20	44.66	60.11	85.36	131.8
FM (RS)	1.1	--	--	--	--	--
Coll (ref 1)	1.5	8.632	11.31	15.24	21.82	34.29
Coll (TS)	1.5	8.604	11.25	15.20	21.69	33.65
BIE	1.5	8.634	11.29	15.27	21.90	34.60
FM (ARF)	1.5	8.560	11.26	15.33	22.09	34.77
FM (RS)	1.5	--	9.501	12.90	18.60	--
Coll (ref 1)	2.0	5.309	6.996	9.565	13.88	22.14
Coll (TS)	2.0	5.386	7.024	9.557	13.84	22.04
BIE	2.0	5.270	6.966	9.545	13.86	22.13
FM (ARF)	2.0	5.247	6.976	9.631	14.08	22.46
FM (RS)	2.0	--	--	--	--	--

$$\frac{E'B\Delta_{cm}W}{6M}$$

Method	r_2/r_1	a/W				
		0.3	0.4	0.5	0.6	0.7
Coll (ref 1)	1.1	2.191	3.714	6.314	10.96	22.40
Coll (TS)	1.1	--	--	--	--	--
BIE	1.1	2.274	3.803	6.431	11.51	23.16
FM (ARF)	1.1	2.126	3.570	6.014	10.60	20.58
FM (RS)	1.1	--	--	--	--	--
Coll (ref 1)	1.5	2.219	3.620	6.194	11.04	22.02
Coll (TS)	1.5	2.177	3.650	6.152	10.97	21.80
BIE	1.5	2.252	3.709	6.223	11.30	22.20
FM (ARF)	1.5	2.184	3.661	5.991	10.49	20.34
FM (RS)	1.5	--	3.598	5.986	10.46	--
Coll (ref 1)	2.0	2.229	3.661	6.115	10.85	21.67
Coll (TS)	2.0	2.275	3.704	6.183	10.88	21.63
BIE	2.0	2.216	3.621	6.054	10.78	21.61
FM (ARF)	2.0	2.226	3.605	5.935	10.34	20.05
FM (RS)	2.0	--	--	--	--	--

TABLE II. (CONT'D)

$$\frac{E'B\Delta_{total}}{P}$$

Method	r_2/r_1	a/W				
		0.3	0.4	0.5	0.6	0.7
Irwin's Eq.	1.1	1013	1182	1470	2007	3199
Coll (TS)	1.1	--	--	--	--	--
BIE	1.1	924.2	853.0	1073	1489	2413
FM (ARF)	1.1	712.3	832.2	1037	1412	2199
FM (RS)	1.1	--	--	--	--	--
Irwin's Eq.	1.5	26.13	36.59	54.79	89.77	170.5
Coll (TS)	1.5	14.61	20.13	30.54	49.54	90.92
BIE	1.5	14.91	20.63	30.70	50.16	94.21
FM (ARF)	1.5	15.23	20.78	30.32	48.24	87.17
FM (RS)	1.5	--	35.67	53.01	85.65	--
FM (RS,rel)	1.5	--	20.67	30.20	48.02	--
Irwin's Eq.	2.0	8.99	12.97	20.02	33.97	67.24
Coll (TS)	2.0	5.10	6.60	9.42	14.77	27.87
BIE	2.0	4.80	6.33	9.09	14.70	27.60
FM (ARF)	2.0	5.42	6.93	9.58	14.72	26.30
FM (RS)	2.0	--	--	--	--	--

Coll (ref 1) - Collocation reference 1
Coll (TS)   - Collocation this study
BIE   - Boundary integral equation
FM (ARF)   - Finite element with physical load point fixed and roller
               reaction applied at the inside radius
FM (RS)   - Finite element with load applied at the physical load point
               and the inside radius constrained at θ_0
Irwin's Eq. - Irwin's equation
FM (RS,rel) - Finite element with load applied at the physical load point
               and the inside radius constrained at θ_0, relative
               displacement of the load point with respect to the roller
               reaction point

10

TABLE III. NUMERICAL SOLUTIONS FOR THE ARC BEND-ARC SUPPORT SAMPLE WITH $\theta_0 = 54$ DEGREES

$$\frac{KB\sqrt{W}}{P \tan \theta_0}$$

Method	r_2/r_1	a/W				
		0.3	0.4	0.5	0.6	0.7
Coll (ref 1)	1.1	35.28	45.32	60.37	84.70	130.9
Coll (TS)	1.1	--	--	--	--	--
BIE	1.1	35.86	46.62	62.29	88.11	138.1
FM (ARF)	1.1	34.62	45.16	60.67	85.98	132.5
FM (RS)	1.1	--	--	--	--	--
Coll (ref 1)	1.5	8.987	11.71	15.69	22.30	34.82
Coll (TS)	1.5	9.063	11.71	15.70	22.28	34.80
BIE	1.5	9.006	11.73	15.78	22.51	35.42
FM (ARF)	1.5	9.039	11.81	15.94	22.76	35.50
FM (RS)	1.5	--	9.501	13.33	19.06	--
Coll (ref 1)	2.0	5.700	7.432	10.03	14.38	22.68
Coll (TS)	2.0	5.657	7.393	10.01	14.34	22.48
BIE	2.0	5.675	7.418	10.06	14.44	22.85
FM (ARF)	2.0	5.738	7.534	10.24	14.74	23.19
FM (RS)	2.0	--	--	--	--	--

$$\frac{E'B\Delta_{cm}W}{6M}$$

Method	r_2/r_1	a/W				
		0.3	0.4	0.5	0.6	0.7
Coll (ref 1)	1.1	2.209	3.744	6.363	11.02	22.53
Coll (TS)	1.1	--	--	--	--	--
BIE	1.1	2.310	3.867	6.541	11.71	23.60
FM (ARF)	1.1	2.144	3.602	6.067	10.68	20.70
FM (RS)	1.1	--	--	--	--	--
Coll (ref 1)	1.5	2.302	3.780	6.428	11.38	22.56
Coll (TS)	1.5	2.370	3.866	6.443	11.41	22.58
BIE	1.5	2.343	3.861	6.467	11.50	22.91
FM (ARF)	1.5	2.261	3.738	6.217	10.85	20.92
FM (RS)	1.5	--	3.739	6.212	10.81	--
Coll (ref 1)	2.0	2.389	3.916	6.503	11.43	22.55
Coll (TS)	2.0	2.332	3.833	6.408	11.33	22.36
BIE	2.0	2.383	3.885	6.485	11.41	22.63
FM (ARF)	2.0	2.341	3.809	6.273	10.89	20.93
FM (RS)	2.0	--	--	--	--	--

TABLE III. (CONT'D)

$$\frac{E'B\Delta_{total}}{P}$$

Method	r_2/r_1	a/W				
		0.3	0.4	0.5	0.6	0.7
Irwin's Eq.	1.1	5407	6025	7073	9018	13320
Coll (TS)	1.1	-	-	-	-	-
BIE	1.1	2656	2999	3589	4701	7168
FM (ARF)	1.1	2595	2914	3455	4444	6516
FM (RS)	1.1	-	-	-	-	-
Irwin's Eq.	1.5	115.8	156.4	226.0	357.9	657.6
Coll (TS)	1.5	43.28	58.40	86.06	139.3	257.6
BIE	1.5	43.86	60.12	88.23	142.6	262.8
FM (ARF)	1.5	43.79	59.44	86.12	135.6	241.9
FM (RS)	1.5	-	151.4	218.0	341.9	-
FM (RS,rel)	1.5	-	59.26	85.87	135.1	-
Irwin's Eq.	2.0	36.68	52.98	81.23	135.6	262.0
Coll (TS)	2.0	11.08	15.95	23.50	39.39	75.05
BIE	2.0	11.29	15.93	24.14	40.19	76.91
FM (ARF)	2.0	11.69	16.21	24.05	38.92	71.58
FM (RS)	2.0	-	-	-	-	-

Coll (ref 1) - Collocation reference 1
Coll (TS)   - Collocation this study
BIE   - Boundary integral equation
FM (ARF)   - Finite element with physical load point fixed and roller
                reaction applied at the inside radius
FM (RS)   - Finite element with load applied at the physical load point
                and the inside radius constrained at θ_0
Irwin's Eq.   - Irwin's equation
FM (RS,rel)   - Finite element with load applied at the physical load point
                and the inside radius constrained at θ_0, relative displacement
                of the load point with respect to the roller reaction point

DISCUSSION OF NUMERICAL RESULTS

Considering the results for θ_0 = 36 degrees, we find that all of the K

results generated in this study agree with the solutions reported in Reference 1

very well. The maximum difference appears to be about 3 percent in some cases

with most of the solutions being closer if the specimen is modeled by applying

12

the roller reaction as the active load and fixing the load point or the crack

tip. If the specimen is modeled by applying the physical load at the physical

load point and fixing the inside radius at θ_0 to move only in the direction of

θ_0 FM (RS), K does not agree at all with the solution reported in Reference 1.

This finite element model predicts that the stress intensity factor should be

about 18 percent less than that reported in Reference 1 and developed here using

the other model. Considering the crack-mouth-opening displacements, all of the

solutions generated agree with one another quite well, including both finite

element solutions, although for deep cracks, the finite element solutions both

seem to predict less displacement than the other methods.

The major discrepancies occur with the load-line displacements. Using

Irwin's Equation to predict the load-line displacement solution by integrating

the K solutions in Reference 1, a much greater load-line displacement is pre-

dicted than if the specimen is modeled with the roller support reaction applied

and the physical load point or the crack tip is fixed. The difference can be

greater than 50 percent. Furthermore, all of the numerical solutions developed

here agree with one another (within about 4 percent). The interesting discovery

here is that when the specimen is modeled such that the active load is applied

at the physical load point and the inside radius is constrained at θ_0 in the

direction of θ_0, the finite element solution agrees with Irwin's Equation and

disagrees with the other numerical solutions. An additional solution is pre-

sented for the load-line displacements: the specimen is modeled by applying the

load at the physical load point and constraining at θ_0 in the direction of θ_0,

but determines the displacement of the load point relative to the roller reac-

tion point FM (RS,rel). This relative displacement agrees with the solutions

generated by fixing the load point and applying the roller reaction as the

13

active load. This observation suggests that both the numerical solutions and the Irwin's Equation solutions are correct, but solve for a different parameter.

The discrepancy between the two solution methods is unusual and unexpected. The two models for the specimen are statically equivalent, i.e., from a mechanics of materials approach, they should produce the same solutions. For K and Δ_{cm}, the same solution is obtained regardless of modeling. This would lead one to believe that the load-line displacements generated with these models should be very accurate. As it turns out, they are indeed accurate to determine the displacement of the reaction point relative to the load point, but it is clear that there is another component of the load-line displacement that is not accounted for. This additional displacement in the direction of the load-line at first suggests that a general translation of the specimen must occur, but of course that is impossible with the static conditions that must apply. Rather, the additional displacement is a consequence of the imposed conditions that the specimen cannot move in the θ_0 direction. This condition can be met with the reaction point moving in the direction of the applied load if there is additional displacement in the direction perpendicular to the load-line direction such that the vector sum of these displacements is zero in the θ_0 direction. Such a constraining condition is easily applied to a computer stress analysis, but may be very difficult to produce in the laboratory. In the laboratory, the conditions for supporting the arc bend-arc support sample would be to fix the roller location parallel and perpendicular to the direction of the applied load in some sort of a bearing such that roller rotation is allowed. When the load is applied to maintain the condition that the displacement in the direction of θ_0 is zero, the rollers must move in the direction of the applied load so that

the initial point of roller contact remains the only point of contact. Since the rollers would normally be fixed in space, the additional displacement must be accommodated by the specimen moving relative to the rollers. This changes the boundary conditions making the specimen in actual testing nonlinear in the sense that the boundary conditions are variable (θ_0 changes with the magnitude of applied load and crack length). Of course, if the loads are low and the resulting displacements of the specimen are also small, the laboratory conditions are close to the idealized boundary conditions outlined. This suggests that if the specimen is to be used on a material with properties such that relatively large displacements will result, the arc bend-arc support specimen is of questionable applicability. Such conditions may only be obtained when testing very high strength brittle materials. Use of this specimen for J testing, K-R testing, or even K_{Ic} testing (where as much as 2 percent crack growth is allowed) may not be prudent due to the large displacements involved.

The discrepancy in the K solutions with modeling is also very confusing. As stated, the two models for the specimen are statically equivalent. Therefore, the stresses produced by either loading condition should be the same. Of the three specimen parameters presented in this report, K should be the parameter most closely associated with stress. Therefore, it would be expected that the parameter most insensitive to modeling should be K. This is apparently not the case. A possible explanation is that the additional displacement introduced by the idealized boundary conditions would cause the resultant bending stress on the uncracked ligament to change. If the stress on the uncracked ligament changes, certainly the stress intensity factor could change.

EXPERIMENTAL PROCEDURE

Experimental measurements of load-line compliances for the arc bend-arc support sample in several possible specimen geometries were obtained. Two sets of experiments were run. In the first, as shown in Figure 3, great pains were taken to position the fixtures of the reaction rollers. As shown in the figure, the rollers were fixed in space, but were supported in bearings such that free rotation of the supports was allowed. Although not shown in Figure 3, the columns supporting the rollers and bearings were stiffened during testing in the horizontal direction to minimize lateral deflection of the fixture. In the second study, the rollers were positioned as suggested in ASTM Standard E-399 on Fracture Toughness Testing of Metallic Materials. In this second case, the rollers are fixed such that they cannot move in the direction of the applied load, but are free to move perpendicular to the direction of the applied load. This is another way to accommodate rotation of the roller supports. Also, in the first study, cracks were approximated by machined saw cuts or by fatigue cracking, while in the second group of experiments, the cracks were produced by fatigue cracking only. The material used in the first study was a brittle martensitic steel whose properties are presented in Reference 8. In the second study, the material was ASTM A723 Grade 2, Class 3, pressure vessel steel. The results from the first experimental study are discussed first.

A typical load versus load-line displacement plot from an autographic plotter is shown in Figure 4 for the case of the rollers fixed in space and supported on bearings. As can be seen from the plot, there is both some hysteresis and nonlinearity in the load-displacement behavior. For those tests performed with the rollers fixed in space and supported in bearings, the nonlinearity and hysteresis were smoothed by using least squares to determine the compliance. The data shown in Figure 4 were digitized and the analysis was performed.

16

The results for two specimens over a wide range of crack depths are given in Figure 5. In this plot, k is the radius ratio r_2/r_1. Also, the experimental results are compared with various predictions of the load-line compliance. For each crack depth tested, there are three points plotted in the figure: the highest recorded compliance, the lowest recorded compliance, and the average of all the measurements. Usually there were five loadings and unloadings for each experimental condition. The solid line in the figure is the Irwin's Equation prediction of compliance from Table I for the case of k = 1.25 and θ_0 = 45 degrees. This solution agrees quite well with the experimentally-determined compliances at all crack depths studied. The dashed line is the Irwin's Equation solution for k = 1.5 and θ_0 = 54 degrees. The agreement between this prediction and the experimentally-determined compliances is also very good except when the normalized crack depth is either 0.1 or 0.5, where the experimental data are 22 percent and 40 percent, respectively, higher than the predicted data. All possible explanations for this discrepancy were explored without success. Also shown in this figure are the finite element predictions for k = 1.5 and θ_0 = 54 degrees using both models of analysis. It is clear that the predictions using Model 1 (the load point fixed and the reaction load actively applied) do not agree at all with the experimental results, but the results obtained using Model 2 (the load actively applied and the reaction points fixed in the θ_0 direction) do indeed agree with the experimental results.

A second series of tests was performed using the fixturing shown in Figure 3 on actual fatigue precracked K_{Ic} samples (ref 9). The load-line compliance results for these specimens are shown in Figure 6. Two specimen geometries were studied here, one with k = 1.20 and the other with k = 1.25. In both of these cases, the agreement with the Irwin's Equation prediction of compliance was very good.

Another series of tests was performed with a precracked sample of ASTM A723 pressure vessel steel with the condition that $k = 2.0$ and $\theta_0 = 36$ degrees with the rollers supported as presently suggested in ASTM Standard E-399. Typical load versus load-line displacement traces obtained from this study are shown in Figure 7. When these results are compared with the traces given in Figure 4, it is clear that with these types of supports, more nonlinearity is induced and there is a greater amount of hysteresis behavior. In this case, both of these observations are to be expected due to increased roller friction. The load-line compliances from this testing were determined graphically by taking the slope of the most linear portion of the load displacement trace. The measured compliances appear in Figure 8. Also shown in the figure are the Irwin's Equation prediction and the finite element prediction using Model 1 (load point fixed and the roller reactions actively applied). The comparisons are quite interesting. When the crack length is small and the specimen is stiff, the measured compliances are in good agreement with the Irwin's Equation prediction. When the crack gets a little deeper and the specimen gets more compliant, the specimen must move relative to the rollers. Since the amount of relative motion of the specimen with respect to the rollers is restricted because of roller friction, the measured compliances deviate from the Irwin's Equation prediction and follow the finite element, Model 1 prediction, for a time. Finally, when the crack is very deep and the specimen is very compliant, the roller friction severely limits the specimen's compliance. At the very deep crack depths, significant plastic deformation at the roller supports was observed.

These experimental results suggest that when small amounts of displacement are expected, the specimen will deform according to the Irwin's Equation prediction. In order for this to occur, the specimen must be free to move relative to

18

the rollers. When the rollers restrict this relative motion, the only displacement that is observed is the motion of the roller support location relative to the load-point motion. And finally, if the specimen is very compliant, pin friction can drastically change the compliance response.

REFERENCES

1. B. Gross and J.E. Srawley, "Stress Intensity and Displacement Coefficients for Radially Cracked Ring Segments Subject to Three-Point Bending," NASA TM 83059, National Aeronautics and Space Administration, Washington, D.C., March 1983.

2. A.T. Jones, "Fracture Toughness Testing With Sections of Cylinders," Engineering Fracture Mechanics, Vol. 6, No. 4, 1974, pp. 653-662.

3. G.R. Irwin and J.A. Kies, "Fracturing and Fracture Dynamics," Welding Journal Research Supplement, Vol. 31, 1952.

4. G.R. Irwin, "Analysis of Stresses and Strains Near the End of a Crack Transversing a Plate," Journal of Applied Mechanics, Vol. 24, 1957, p. 361.

5. L.N. Gifford, Jr. and P.D. Hilton, "Stress Intensity Factors by Enriched Finite Elements," Engineering Fracture Mechanics, Vol. 10, No. 3, 1978, pp. 485-496.

6. B. Gross, E.J. Roberts, and J.E. Srawley, "Elastic Displacements for Various Edge-Cracked Plate Specimens," International Journal of Fracture Mechanics, Vol. 4, No. 3, September 1968, pp. 267-276 (Errata, Vol. 6, 1970, p. 87).

7. J.O. Watson, "Hermitian Cubic Boundary Elements for Plane Problems of Fracture Mechanics," Res Mechanica, Vol. 4, No. 1, 1982, pp. 23-42.

8. D.S. Saunders and F.I. Baratta, "The Measurement of Fracture Toughness of Steels From the M795 and M549 Artillery Projectiles Using Small Sized Fracture Toughness Specimens," MTL TR 86-22, U.S. Army Materials Technology Laboratory, Watertown, MA, June 1986.

9. F.I. Baratta and D.S. Saunders, "Comparative Evaluation of LAW Motor Bodies of Three Materials," AMMRC TR 98-7, Watertown, MA, May 1985.

Figure 1a. Arc-shaped bending samples.

Figure 1b. Arc bend-chord support.

21
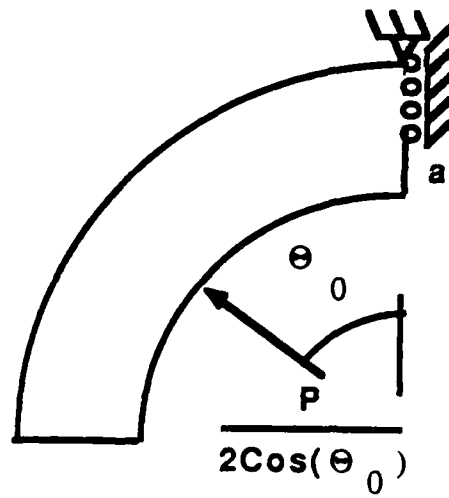
Figure 2a.   Arc bend-arc support.
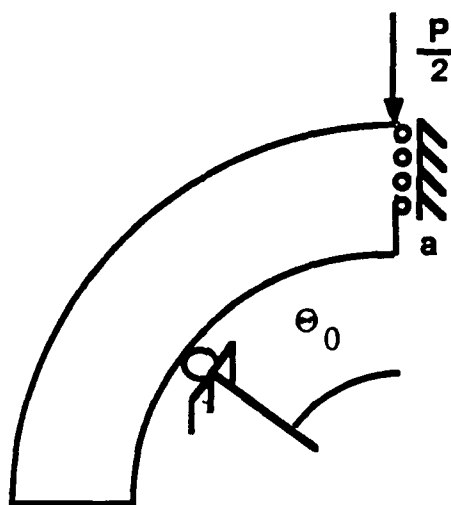
Figure 2b.   Two models used to analyze the
arc bend-arc support specimen.

22
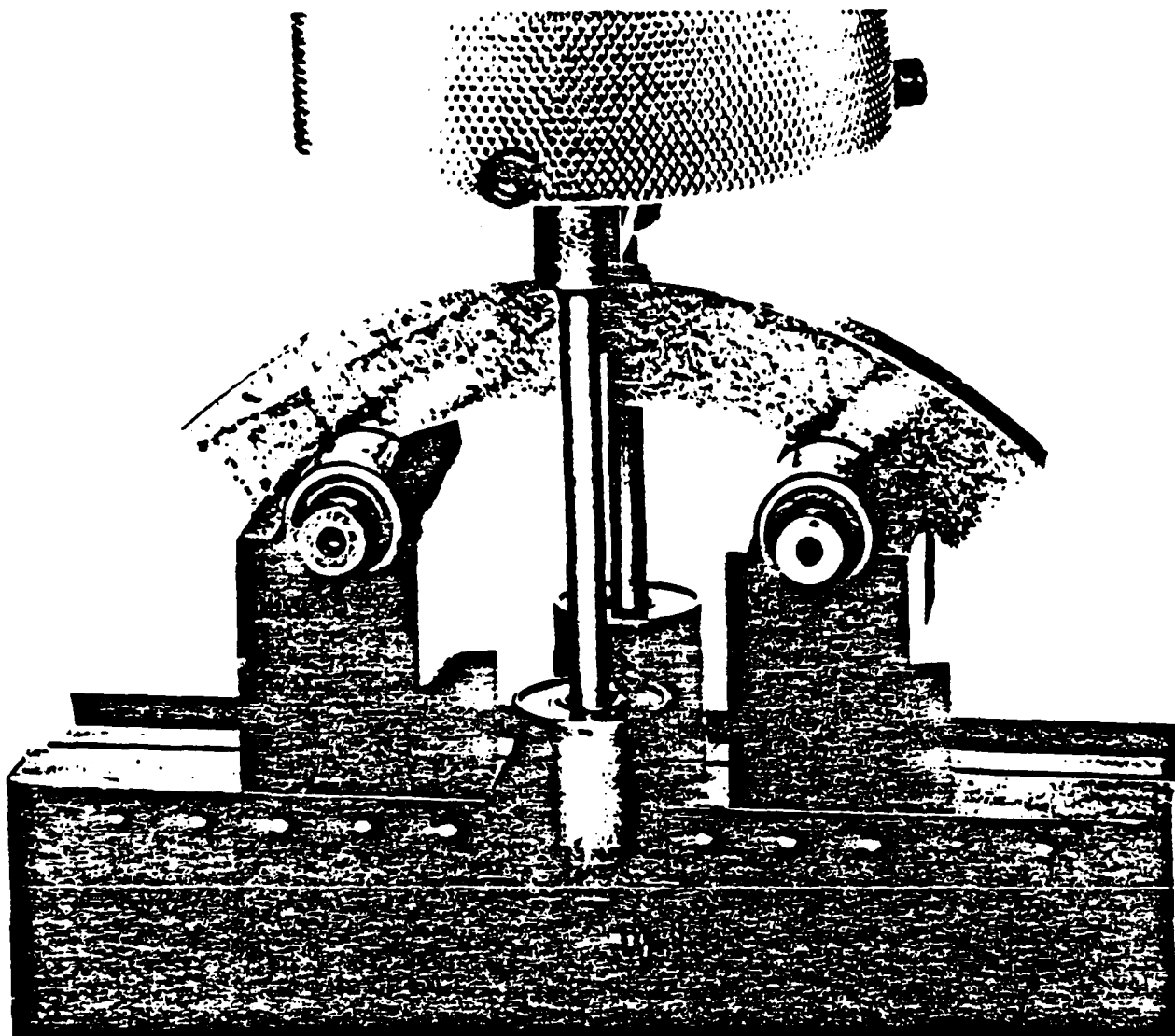
Figure 3. Experimental arrangement with rollers
fixed in space and supported on bearings.
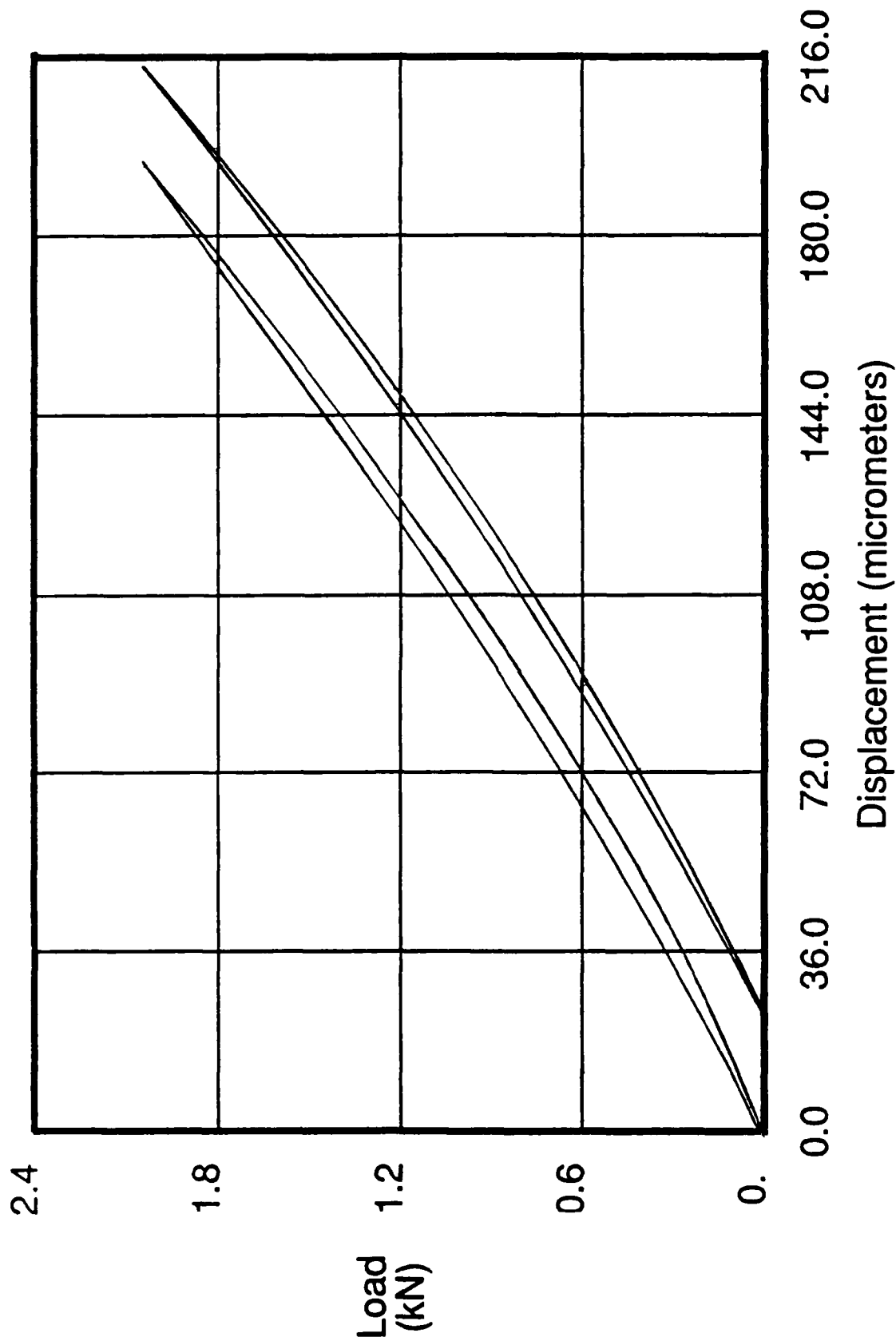
Figure 4. Typical load-line displacement versus applied load traces when using the experimental arrangement in Figure 3. The radius ratio is 1.5, θ_0 is 54 degrees, and a/W is 0.2.

24
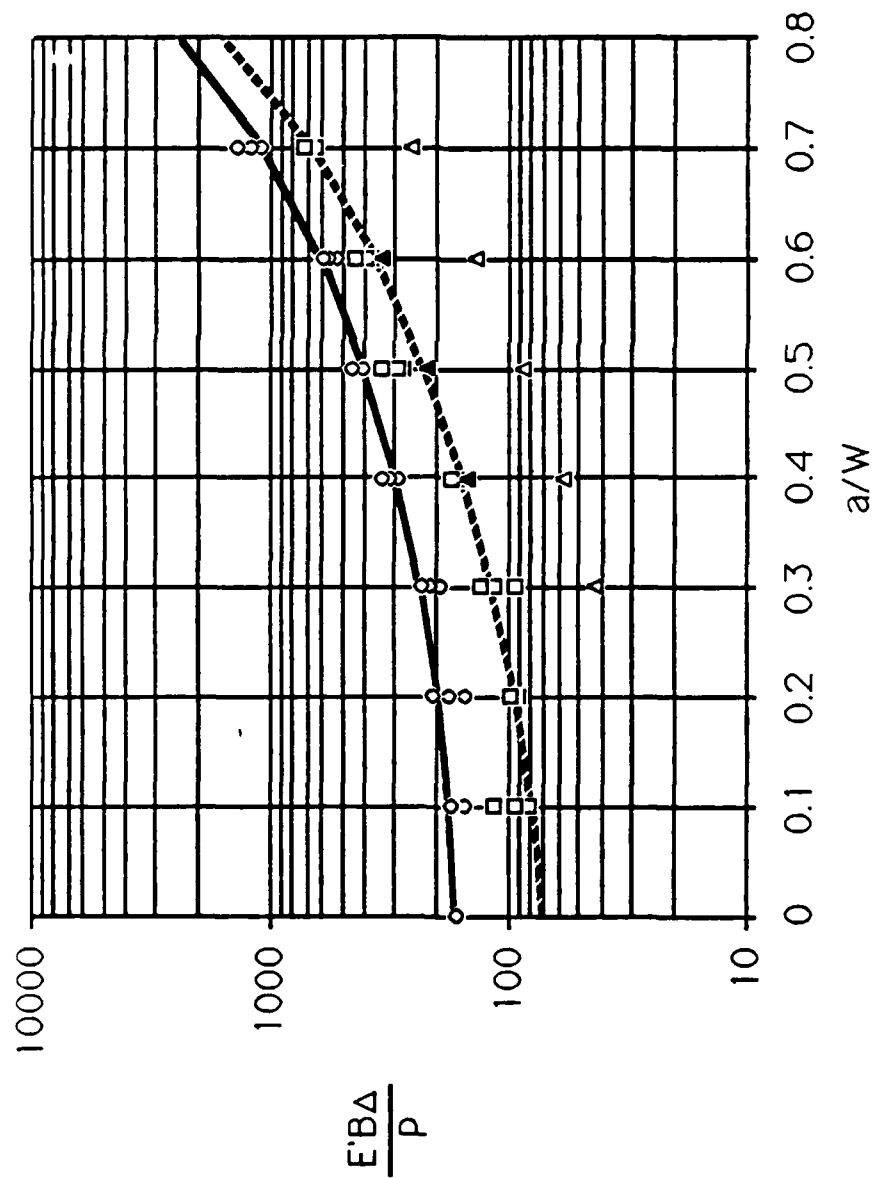
Figure 5. Comparison of experimentally measured load-line compliances obtained with the arrangement in Figure 3 with predicted load-line compliances. The cracks are machined in the specimen.

The legend for the figure is as follows:

- k=1.25, Theta Zero=45°, Irwin's Equation
- k=1.25, Theta Zero=45°, Experimental
- k=1.5, Theta Zero=54°, Irwin's Equation
- k=1.5, Theta Zero=54°, Experimental
- k=1.5, Theta Zero=54°, Finite Element Model 2
- k=1.5, Theta Zero=54°, Finite Element Model 1

The vertical axis is $\frac{E'B\Delta}{P}$ ranging from 10 to 10000. The horizontal axis is a/W ranging from 0 to 0.8.

25
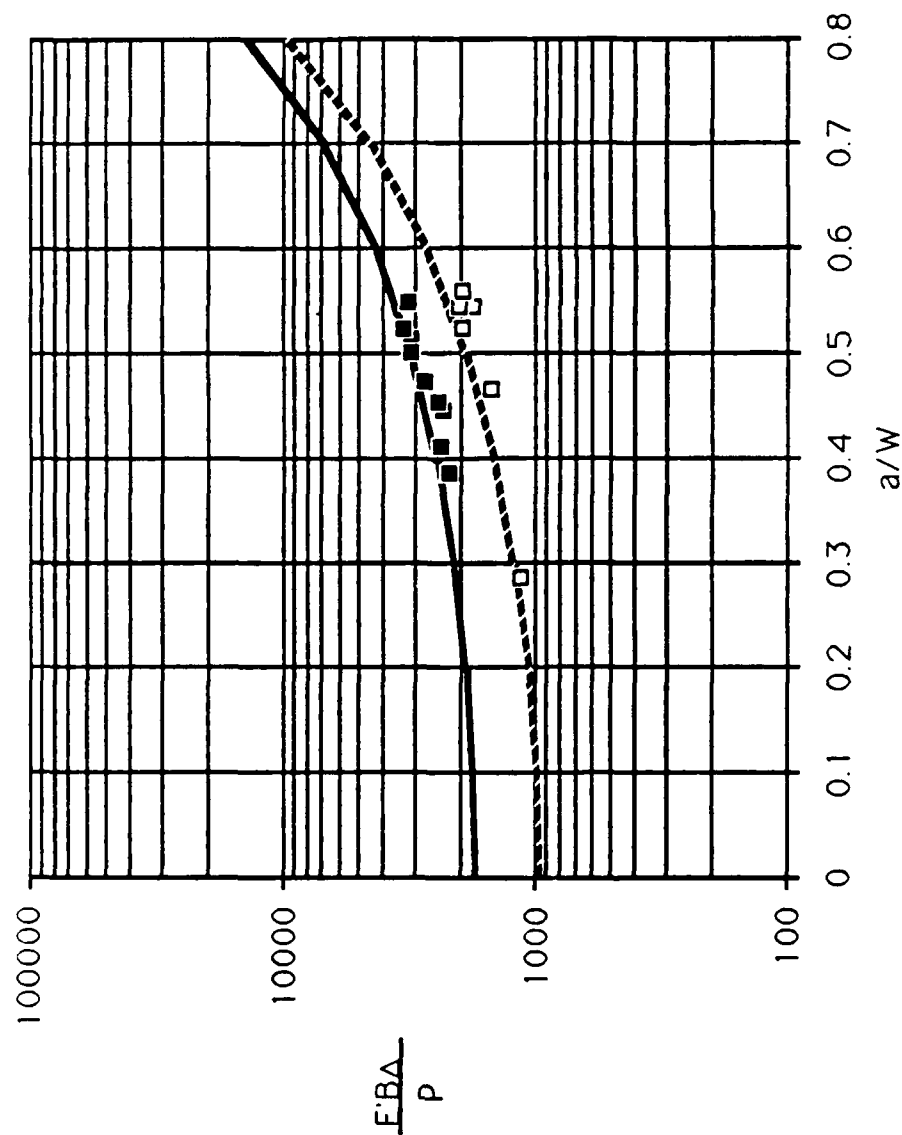
Figure 6. Comparison of experimentally measured load-line compliances obtained with the arrangement in Figure 3 with predicted load-line compliances. The cracks are from fatigue precracking.
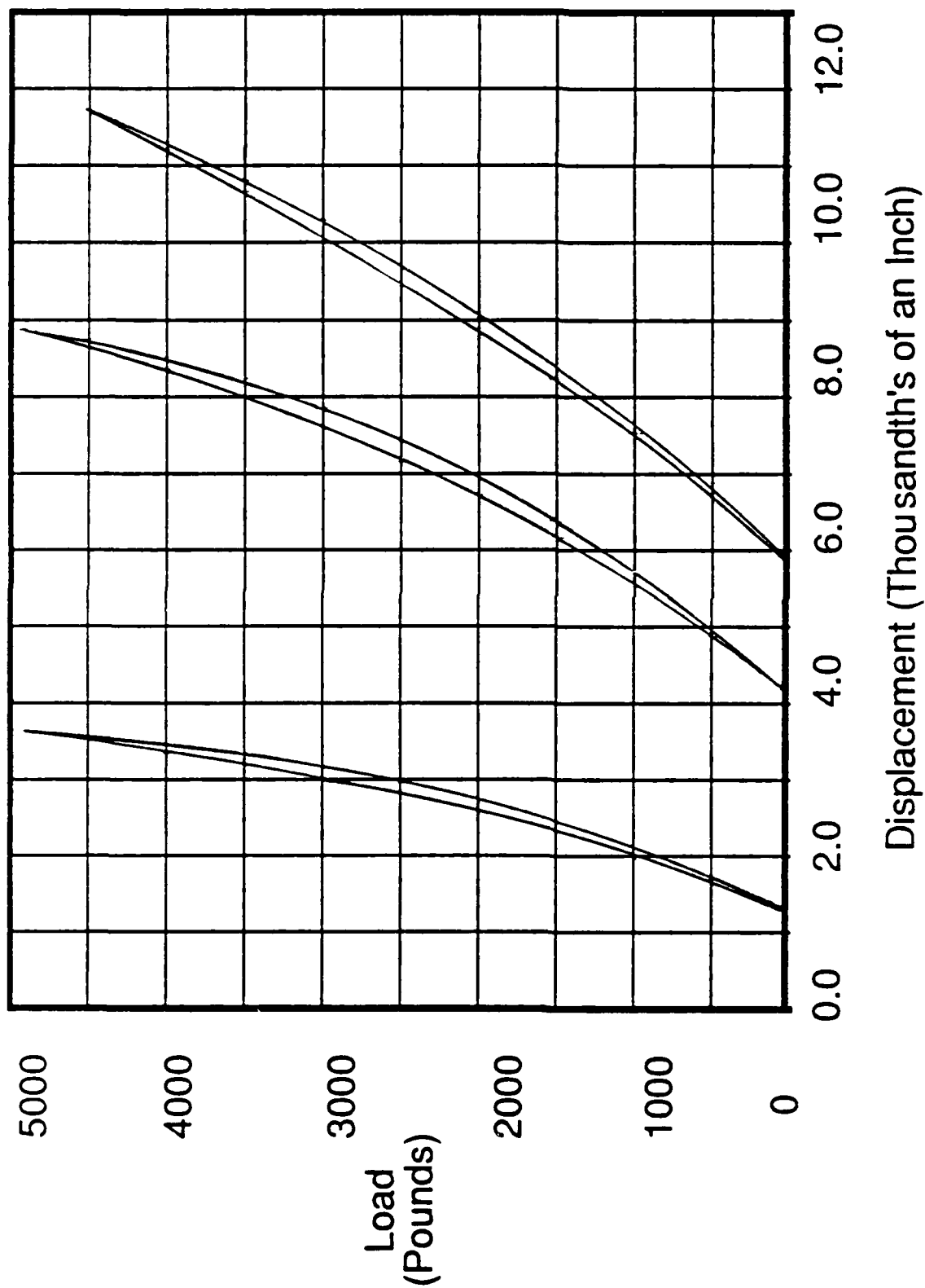
Figure 7. Typical load-line displacement versus applied load traces when using the experimental arrangement for three-point bending samples suggested in ASTM Standard E-399. The radius ratio is 2.0, ϑ_0 is 36 degrees, and the normalized crack lengths are (from left to right) 0.35, 0.45, and 0.55, respectively.
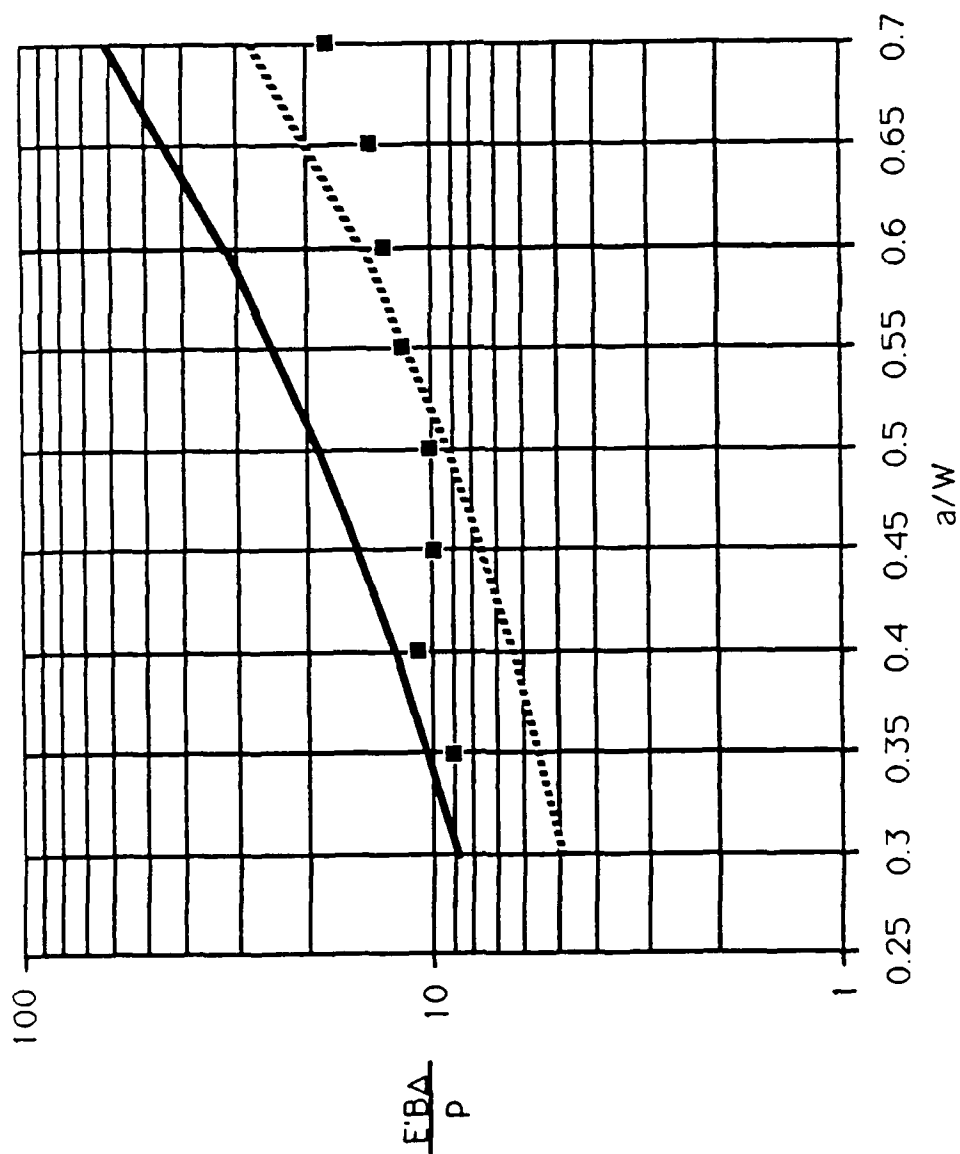
Figure 8. Comparison of experimentally measured load-line compliances with prediction using the experimental arrangement for three-point bending samples suggested in ASTM Standard E-399.

28

APENDIX A

LOAD-LINE COMPLIANCES FOR ARC BEND-ARC SUPPORT SAMPLES WITH EXTERNAL CRACKS

An additional sample that has been suggested is the arc bend-arc support sample with the crack on the external surface. This specimen is the same basic geometry as shown in Figure 1b, except that the crack and roller supports are on the outside diameter of the specimen, and the load is applied at mid-span on the inside diameter of the specimen. The stress intensity factor and crack-mouth-opening displacement solutions for this sample have been developed using collocation (ref 1). It is a relatively simple matter to apply the Irwin's Equation approach to this sample to predict its load-line compliance. In the course of the work presented in the main body of this report, the analysis of the externally cracked arc bend-arc support sample was performed. The equation for Δ_{no} crack is easily determined using Winkler's theory and the expression is

$$
\Delta_{no} \text{ crack} = \frac{P}{BE} \left\{ \frac{k+1}{8(k-1)} \left[\left(\frac{\theta_0}{\cos^2 \theta_0} - \tan \theta_0 \right) / \left(1 - \frac{2(k-1)}{(k+1)\ln(k)} \right) + \frac{3(2+\mu)\theta_0}{\cos^2 \theta_0} \right. \right.
$$

$$
\left. \left. + 3\mu\tan \theta_0 \right] \right\} \tag{A1}
$$

The contribution of the crack to the deflection (Δ_{crack}) was determined as described in the main body of the report (Eqs. (5), (6), and (7)). The only difference here is that the interpolating polynomials (Eq. (7)) were fit to the numerical stress intensity factors for externally cracked arc bend-arc support samples from Reference 1. The results of the integration are given in Table A-I.

TABLE A-I. $EB\Delta_{total}/P$ DETERMINED USING IRWIN'S EQUATION APPROACH FOR AN EXTERNALLY CRACKED SAMPLE

$r_2/r_1 = 1.1$

a/W θ_0	11.46	18	27	36	45	54	63	72	81
0.0	23.32	84.75	303.6	829.1	2012	4743	11810	35240	179600
0.1	24.93	89.04	314.3	851.3	2054	4823	11970	35640	183300
0.2	28.32	98.12	337.3	898.6	2145	4996	12320	36510	185000
0.3	34.45	114.7	379.5	985.9	2311	5315	12970	38120	191800
0.4	44.89	143.0	451.3	1134	2595	5856	14080	40860	203400
0.5	62.93	191.6	574.3	1387	3078	6779	15960	45510	223100
0.6	96.92	282.4	802.8	1856	3973	8486	19440	54210	259400
0.7	172.6	483.0	1305	2884	5929	12220	27010	72810	338500
0.8	387.6	1050	2719	5776	11420	22690	48240	125100	560200

$r_2/r_1 = 1.15$

a/W θ_0	13.5	18	27	36	45	54	63	72	81
0.0	13.49	29.47	100.8	270.4	650.3	1526	3788	11290	57470
0.1	14.45	31.29	105.4	280.0	668.7	1561	3859	11460	58220
0.2	16.49	35.20	115.5	300.9	709.0	1638	4018	11860	59880
0.3	20.22	42.38	134.1	339.7	783.6	1781	4311	12580	62960
0.4	26.60	54.58	165.6	405.5	710.2	2023	4809	13820	68170
0.5	37.55	75.47	219.5	517.3	1125	2433	5652	15900	76900
0.6	58.14	114.4	319.2	723.5	1521	3186	7200	19720	93130
0.7	104.1	200.5	538.2	1174	2384	4824	10570	28020	128100
0.8	236.6	446.5	1160	2449	4819	9435	20050	51330	226400

$r_2/r_1 = 1.20$

a/W θ_0	13.5	18	27	36	45	54	63	72	81
0.0	7.170	14.81	48.06	126.2	300.3	700.4	1732	5149	26180
0.1	7.710	15.84	50.69	131.7	310.8	720.6	1773	5251	26610
0.2	8.820	17.99	56.28	143.3	333.4	763.9	1802	5472	27550
0.3	10.82	21.89	66.52	164.8	374.9	843.8	2027	5881	29280
0.4	14.24	28.57	83.98	201.5	445.8	980	2306	6578	32230
0.5	20.21	40.10	114.0	264.1	566.7	1212	2783	7763	37240
0.6	31.50	61.71	169.7	379.9	789.7	1638	3657	9939	46420
0.7	56.57	109.2	291.0	630.2	1271	2556	5537	14610	66080
0.8	126.7	240.8	625.0	1316	2586	5062	10660	27350	119500

$r_2/r_1 = 1.25$

θ_0 a/W	18	27	36	45	54	63	72	81
0.0	9.10	27.47	71.71	168.6	390.6	961.9	2852	14470
0.1	9.73	29.62	75.17	175.3	403.4	988.2	2917	14750
0.2	11.07	33.16	82.63	189.7	431.3	1046	3059	15350
0.3	13.51	39.65	96.38	216.4	482.7	1152	3324	16480
0.4	17.67	50.7	119.8	246.7	570.1	1333	3772	18390
0.5	24.84	69.6	159.6	338.7	718.4	1639	4532	21620
0.6	38.29	104.2	233.0	480.1	990.2	2200	5921	27520
0.7	68.08	181.4	392.8	780.4	1577	3412	8911	40190
0.8	152.5	396.4	837.7	1635	3201	6762	17160	75110

$r_2/r_1 = 1.50$

θ_0 a/W	27	36	45	54	63	72	81
0.0	6.71	15.33	33.73	75.09	180.3	525.5	2637
0.1	7.10	16.17	35.40	78.34	187.0	542.4	2709
0.2	7.94	18.00	39.02	85.41	201.8	579.5	2868
0.3	9.48	21.37	45.71	98.52	229.2	648.4	3163
0.4	12.10	27.10	57.12	120.8	275.9	765.8	3666
0.5	16.60	36.92	76.56	158.7	355.0	964.4	4514
0.6	25.01	55.05	112.3	228.0	499.4	1326	6054
0.7	43.44	94.40	189.4	376.6	808.5	2099	9329
0.8	94.90	203.2	401	782.9	1651	4202	18200

$r_2/r_1 = 2.00$

θ_0 a/W	31.5	36	45	54	63	72	81
0.0	3.55	4.99	9.96	20.72	47.45	133.8	655.6
0.1	3.70	5.21	10.40	21.59	49.28	138.4	675.6
0.2	4.01	5.68	11.35	23.50	53.31	148.7	720.1
0.3	4.58	6.52	13.09	27.00	60.77	167.8	803.1
0.4	5.92	7.94	16.03	32.91	73.35	200.0	943.3
0.5	7.15	10.35	20.97	42.84	94.45	253.9	1177
0.6	10.16	14.80	30.02	60.88	132.6	350.9	1596
0.7	16.81	24.51	49.51	99.46	213.6	555.7	2476
0.8	35.64	51.74	103.4	205.2	434.1	1110	4844

TABLE A-I.   (CONT'D)

θ_0 / a/W	36	45	54	63	72	81
$r_2/r_1 = 2.50$						
0.0	3.16	5.97	11.90	26.39	72.6	349.6
0.1	3.26	6.17	12.32	27.27	74.9	359.3
0.2	3.47	6.62	13.23	29.23	79.9	381.5
0.3	3.85	7.44	14.91	32.88	89.4	423.2
0.4	4.49	8.81	17.73	39.00	105.2	493.3
0.5	5.57	11.09	22.41	49.14	131.4	609.1
0.6	7.54	15.21	30.81	67.22	177.9	813.6
0.7	11.85	24.08	48.64	105.3	274.9	1239
0.8	24.16	--	97.70	208.9	536.9	2379

TECHNICAL REPORT INTERNAL DISTRIBUTION LIST

	NO. OF COPIES
CHIEF, DEVELOPMENT ENGINEERING DIVISION	
ATTN: SMCAR-CCB-D	1
-DA	1
-DC	1
-DM	1
-DP	1
-DR	1
-DS (SYSTEMS)	1
CHIEF, ENGINEERING SUPPORT DIVISION	
ATTN: SMCAR-CCB-S	1
-SE	1
CHIEF, RESEARCH DIVISION	
ATTN: SMCAR-CCB-R	2
-RA	1
-RM	1
-RP	1
-RT	1
TECHNICAL LIBRARY	5
ATTN: SMCAR-CCB-TL	
TECHNICAL PUBLICATIONS & EDITING SECTION	3
ATTN: SMCAR-CCB-TL	
DIRECTOR, OPERATIONS DIRECTORATE	1
ATTN: SMCWV-OD	
DIRECTOR, PROCUREMENT DIRECTORATE	1
ATTN: SMCWV-PP	
DIRECTOR, PRODUCT ASSURANCE DIRECTORATE	1
ATTN: SMCWV-QA	

NOTE: PLEASE NOTIFY DIRECTOR, BENET LABORATORIES, ATTN: SMCAR-CCB-TL, OF
       ANY ADDRESS CHANGES.

TECHNICAL REPORT EXTERNAL DISTRIBUTION LIST

	NO. OF COPIES			NO. OF COPIES

ASST SEC OF THE ARMY
RESEARCH AND DEVELOPMENT
ATTN: DEPT FOR SCI AND TECH   1
THE PENTAGON
WASHINGTON, D.C. 20310-0103

COMMANDER
ROCK ISLAND ARSENAL
ATTN: SMCRI-ENM   1
ROCK ISLAND, IL 61299-5000

ADMINISTRATOR
DEFENSE TECHNICAL INFO CENTER
ATTN: DTIC-FDAC   12
CAMERON STATION
ALEXANDRIA, VA 22304-6145

DIRECTOR
US ARMY INDUSTRIAL BASE ENGR ACTV
ATTN: AMXIB-P   1
ROCK ISLAND, IL 61299-7260

COMMANDER
US ARMY ARDEC
ATTN: SMCAR-AEE   1
      SMCAR-AES, BLDG. 321   1
      SMCAR-AET-O, BLDG. 351N   1
      SMCAR-CC   1
      SMCAR-CCP-A   1
      SMCAR-FSA   1
      SMCAR-FSM-E   1
      SMCAR-FSS-D, BLDG. 94   1
      SMCAR-IMI-I (STINFO) BLDG. 59   2
PICATINNY ARSENAL, NJ 07806-5000

COMMANDER
US ARMY TANK-AUTMV R&D COMMAND
ATTN: AMSTA-DDL (TECH LIB)   1
WARREN, MI 48397-5000

COMMANDER
US MILITARY ACADEMY   1
ATTN: DEPARTMENT OF MECHANICS
WEST POINT, NY 10996-1792

US ARMY MISSILE COMMAND
REDSTONE SCIENTIFIC INFO CTR   2
ATTN: DOCUMENTS SECT, BLDG. 4484
REDSTONE ARSENAL, AL 35898-5241

DIRECTOR
US ARMY BALLISTIC RESEARCH LABORATORY
ATTN: SLCBR-DD-T, BLDG. 305   1
ABERDEEN PROVING GROUND, MD 21005-5066

COMMANDER
US ARMY FGN SCIENCE AND TECH CTR
ATTN: DRXST-SD   1
220 7TH STREET, N.E.
CHARLOTTESVILLE, VA 22901

DIRECTOR
US ARMY MATERIEL SYSTEMS ANALYSIS ACTV
ATTN: AMXSY-MP   1
ABERDEEN PROVING GROUND, MD 21005-5071

COMMANDER
HQ, AMCCOM
ATTN: AMSMC-IMP-L   1
ROCK ISLAND, IL 61299-6000

COMMANDER
US ARMY LABCOM
MATERIALS TECHNOLOGY LAB
ATTN: SLCMT-IML (TECH LIB)   2
WATERTOWN, MA 02172-0001

NOTE: PLEASE NOTIFY COMMANDER, ARMAMENT RESEARCH, DEVELOPMENT, AND ENGINEERING
        CENTER, US ARMY AMCCOM, ATTN: BENET LABORATORIES, SMCAR-CCB-TL,
        WATERVLIET, NY 12189-4050, OF ANY ADDRESS CHANGES.

	NO. OF COPIES		NO. OF COPIES
COMMANDER US ARMY LABCOM, ISA ATTN: SLCIS-IM-TL 2800 POWDER MILL ROAD ADELPHI, MD 20783-1145	1	COMMANDER AIR FORCE ARMAMENT LABORATORY ATTN: AFATL/MN EGLIN AFB, FL 32542-5434	1
COMMANDER US ARMY RESEARCH OFFICE ATTN: CHIEF, IPO P.O. BOX 12211 RESEARCH TRIANGLE PARK, NC 27709-2211	1	COMMANDER AIR FORCE ARMAMENT LABORATORY ATTN: AFATL/MNF EGLIN AFB, FL 32542-5434	1
DIRECTOR US NAVAL RESEARCH LAB ATTN: MATERIALS SCI & TECH DIVISION CODE 26-27 (DOC LIB) WASHINGTON, D.C. 20375	1 1	METALS AND CERAMICS INFO CTR BATTELLE COLUMBUS DIVISION 505 KING AVENUE COLUMBUS, OH 43201-2693	1

NOTE: PLEASE NOTIFY COMMANDER, ARMAMENT RESEARCH, DEVELOPMENT, AND ENGINEERING CENTER, US ARMY AMCCOM, ATTN: BENET LABORATORIES, SMCAR-CCB-TL, WATERVLIET, NY 12189-4050, OF ANY ADDRESS CHANGES.